

SAR DATA ACQUISITION FOR EVENT-DRIVEN MAPPING OF URBAN AREAS USING GIS

U. Soergel^a, U. Thoennesen^a, U. Stilla^b

^aFGAN-FOM Research Institute for Optronics and Pattern Recognition, Gutleuthausstraße 1, 76275 Ettlingen, Germany

^bPhotogrammetry and Remote Sensing, Technische Universität München, 80290 München, Germany
soe@fom.fgan.de

Commission III, WG VI

KEY WORDS: SAR, Building, Detection, Urban, Simulation, Fusion

ABSTRACT:

Airborne SAR systems allow a flexible ground mapping with high geometric resolution, independent from daytime and weather conditions. This offers the opportunity of using this technology for the analysis of built-up areas. However, the oblique SAR illumination limits the visibility of certain objects in urban areas depending on the viewing direction. Especially at building locations different SAR specific phenomena like layover, shadow, and multipath-propagation burden the interpretation of the SAR imagery even for experts. But, in case of bad viewing conditions, SAR may be the only way to map special events (e.g. flooding, fire, earthquake). In this paper, the benefit of the utilisation of different kinds of GIS data for the SAR mission planning and the analysis of acquired SAR data after such an event are discussed. Simulations based on 3D models of the scene and maps can optimise the SAR data acquisition parameters. In a similar manner fusing the gathered data with the GIS data can support an image interpreter.

1. INTRODUCTION

In general, topographic mapping of urban areas is based on sensor data acquired from airborne platforms in nadir view. The traditional sensors are aerial cameras, detecting passively the reflected light in the visible or near infrared spectral domain of natural illuminated objects in two dimensions. A digital elevation model (DEM) can be derived by stereo analysis from overlapping images. An alternative source of DEM data are LIDAR systems, which illuminate the scene actively with infrared laser pulses and measure the time-of-flight of the backscattered signal. A prerequisite for both methods are good weather conditions.

State-of-the-art high-resolution synthetic aperture radar (SAR) sensors offer an additional mean for high-resolution data acquisition in urban areas. With interferometric methods (InSAR), DEM of the scene can be obtained from two SAR images. In recent years a number of approaches for urban analysis have been proposed, e.g. for building reconstruction [Gamba et al., 2000; Soergel et al., 2003c]. However, the side-looking sensor principle gives rise to different inherent SAR specific phenomena [Schreier, 1993] like layover, radar shadow (occlusion), and multipath-propagation, which burden the data interpretation. Especially in dense built-up areas with high buildings, large portions of the data can be interfered by these effects. Nevertheless, SAR has some advantages compared to other sensor systems. Because of the active scene illumination, SAR is independent of the daytime. The large signal wavelength provides almost insensitivity to weather conditions. The topic of this paper is to describe the usage of GIS data for an event-driven mapping task, which may be requested for traffic monitoring [Stilla et al., 2004], disaster management [Kakumoto et al., 1997] and damage assessment [Shinozuka et al., 2000] in case of a flooding or an earthquake [Takeuchi et al., 2000]. Fig. 1 illustrates the data flow of the integration of GIS data into this task. It is assumed that a high resolution DEM (general mapping) is available, which was taken a-priori

under good weather conditions, e.g. by laser scanning. From the DEM and available map data a 3D scene description is generated [Stilla and Jurkiewicz, 1999], which describes man-made objects by vector data and vegetation by raster data. With this information, the impact of the mentioned SAR phenomena on the visibility of scene objects can be simulated for arbitrary flight path and illumination direction. Depending on the event, simulations of different possible flight trajectories are requested for a selected area of interest. These simulations determine the optimal flight path or set of paths for the mapping of the object class of investigation. After the SAR mission a simulation of the expected effects considering the actual flight path is helpful for the interpretation of the data.

In Chapter 2, the SAR principle and some remote sensing applications of this technique are introduced. The appearance of buildings in radar imagery is discussed in Chapter 3. SAR illumination effects are analysed for an urban scene using GIS data (Chapter 4). Finally, the benefit of the integration of different levels of context information for the interpretation of the acquired SAR imagery is discussed in Chapter 5.

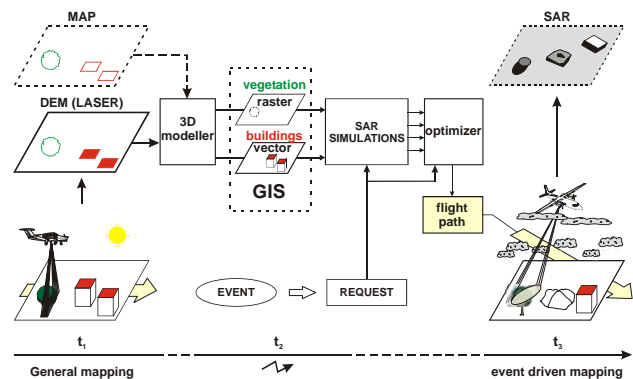


Fig.1 Event-driven SAR data acquisition for urban areas

2. SAR AND INSAR PRINCIPLE

Airborne or spaceborne SAR sensors provide a 2D mapping of the scene in the radar frequency domain. Large areas on the ground are illuminated with radar pulses in an oblique side-looking manner. Because of the larger wavelength λ compared to aerial images, the SAR signal is usually not attenuated by scattering with particles in clouds, smoke or even rain. The choice of a large λ (e.g. 70 cm) even offers the opportunity of penetrating the soil through tree foliage. The range resolution depends on the signal bandwidth. The distance between the sensor and a point target is obtained by correlating the received signal with the complex conjugated transmitted signal [Bamler and Schaettler, 1993]. With this matched filtering all contributions of a certain target can be integrated into the correct range cell. This so-called range compression is carried out for each range bin of the SAR image.

The angular resolution of a radar antenna of aperture D at a range r is approximately $r\lambda/D$. Hence, for remote sensing purposes very large antennas would be required for an appropriate azimuth resolution. This problem is overcome with the synthetic aperture technique. Along the flight path, many overlapping radar measurements are carried out and stored. Each of them can be thought of being collected by one element of a large synthetic array antenna at the same position. In many subsequent measurements the signal of a certain point target is mapped to different ranges cells (range migration). High azimuth resolution is achieved by a coherent integration of these distributed signal contributions to the correct image position. For this purpose, the Doppler frequency is exploited, which is caused from the relative motion between sensor and scene.

The characteristics of the received SAR data depend e.g. on signal properties (wavelength, polarization, transmit power), object properties (e.g. roughness of surface, dielectric constant of material), the distance between sensor and scene (the SNR is indirect proportional to the third power of the range), and the viewing geometry (e.g. the incidence angle). In case of natural scenes, the obtained signal is modelled to be the superposition of the contributions of many independent scatterers inside a resolution cell. In urban scenes, this assumption does not hold everywhere, e.g. due to specular reflection and multi-bounce propagation at building faces and edges. Because of the two-dimensional sinc-curve of the SAR system impulse response, dominant point targets appear as bright stars in the image that may cover the signal of neighboured objects over wide areas. In general, the mapping of a certain urban area is heavily dependent on aspect and elevation angles [Dong et al., 1997].

In urban scenes, the analysis of the SAR scattering matrix [Guillaso et al., 2003] is useful e.g. to discriminate of man-made objects from trees or bushes. However, for this purpose several SAR images of different polarization (e.g. HH, VV and HV) have to be acquired.

For InSAR processing at least two SAR images taken by antennas separated by a baseline orthogonal to the flight directions are required [Rosen et al., 2000]. The different distances of a ground point to the antennas result in a phase difference of the received signals from which a DEM can be calculated. Assuming a constant noise floor, the DEM accuracy varies locally depending mainly on the SNR, which is estimated from the coherence (correlation) of the complex SAR images.

SAR data are acquired in the so-called slant range geometry and have to be orthorectified in a post-processing step. In case of a magnitude SAR image, an external DEM is incorporated for precision geocorrection. InSAR data are orthorectified using the

InSAR DEM, whose local varying accuracy has to be considered for this purpose.

Fig. 2a,b illustrate InSAR magnitude and DEM data covering a part of the test area (Karlsruhe, city centre and University campus). Dark areas of the magnitude image (= poor SNR) coincide with noise in the DEM. The data was acquired from about 5 km distance in the X-band ($\lambda = 3$ cm), range direction is top-down, with off-nadir angle $\theta = 57^\circ$. The geometric resolution is about 1m in range and 0.75m in azimuth direction. The reference LIDAR DEM superimposed with map data is shown in Fig. 2c for comparison.

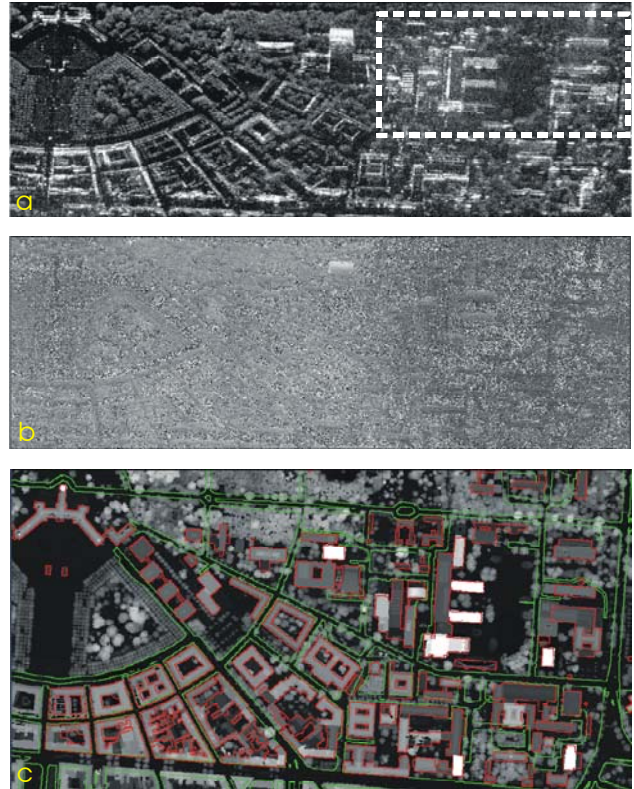


Fig. 2: a,b) InSAR data in slant range (a) magnitude, (b) DEM); c) LIDAR DEM superimposed with building (red) and road layer (green).

3. BUILDINGS IN SAR IMAGERY

For discussion of the appearance of buildings in SAR imagery, the highlighted part of the slant range magnitude image shown in Fig. 2a was transformed into a ground projection (Fig. 3a). Usually a flat scene is assumed for geocoding of SAR images, if no InSAR DEM or external DEM/DTM is available. Fig. 3b shows for comparison the same area of the LIDAR DEM. Both images are overlaid with the map data. The extension of the investigated area is about 400m x 270m.

Buildings appear shifted towards the sensor (range direction is top-down) in the SAR image, e.g. buildings *D* and *E* in the middle. This is caused from the layover effect: because of the side-looking illumination and the wide antenna beam width in elevation, objects located at different positions but with the same distance to the sensor are mapped to the same resolution cell. At building locations a signal mixture from the roof, the walls and the ground is the consequence. If no dominant

scatterers are involved, the signal contributions of different objects can hardly be separated analysing a single SAR image alone. The InSAR DEM is unreliable in layover areas. Layover is a major hindrance for the analysis of SAR data in urban areas, e.g. for building reconstruction.

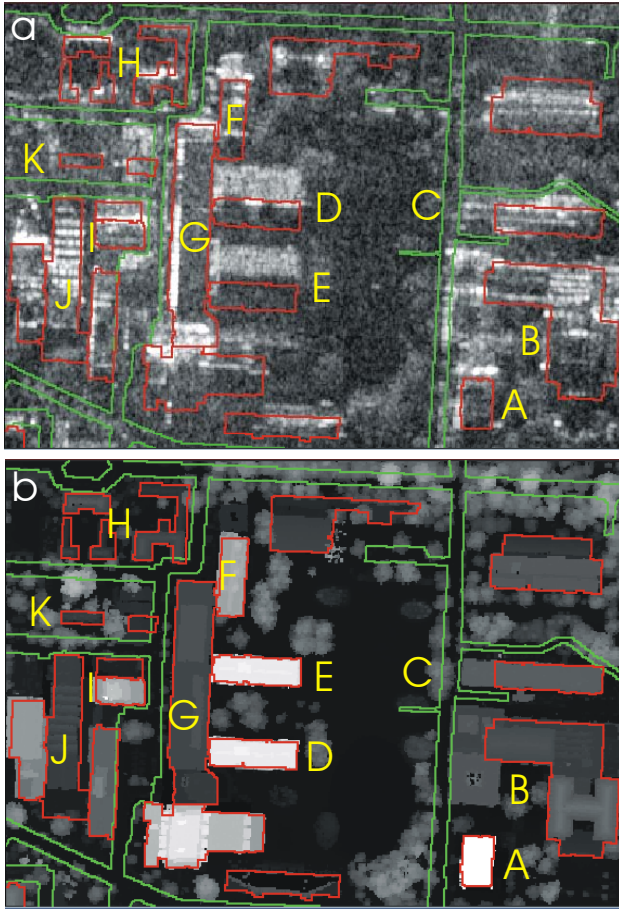


Fig. 3: a) ground range magnitude image and building layer (red); b) DEM and vector map (roads: green).

The choice of a large viewing angle minimizes layover effects. But, large viewing angles lead to extended occlusion areas, caused by the cast shadow from elevated objects on the ground behind. From shadow regions, no signal is returned to the sensor. Therefore, these areas in the SAR data contain no information but noise only. The choice of the viewing angle in a dense urban area is a trade-off between layover and shadow effects [Soergel et al, 2003a].

Since the viewing angle is known, the building height can be determined from the size of layover or shadow areas. However, these features are often disturbed by the signal of other objects. Parallel to the sensor track orientated building walls together with the ground in front of them build a so-called dihedral corner reflector: the signal is reflected back to the sensor by double-bounce scattering. The path length is identical for all double-bounce signals, causing bright lines in azimuth direction in the SAR image located at the building footprints (e.g. at buildings *F* and *G*). At building *I* a dihedral corner is build from the tall main building and the flat roof of the entrance hall.

Another kind of dominant scattering frequently observed in urban areas is specular reflection, e.g. at the roof structures on buildings *B* and *J*. These single-bounce signals can be

discriminated from double-bounce scattering by their polarimetric properties [Guillaso et al., 2003].

In case of a small radar signal wavelength like X-band, there is a significant influence of trees on the visibility of buildings. For example, building *K* is occluded from a large tree, which also covers some small buildings of group *H* in front by layover.

4. CHOICE OF OPTIMAL SAR ACQUISITION PARAMETERS

It is essential to determine a-priori the optimal SAR acquisition parameters in order to minimize the influence of layover and shadow for a selected area of interest or an object class. For this purpose, GIS data are required. Here, we focus on best effort mapping of buildings and roads by SAR for the test area shown in Fig. 3b.

Based on the DEM, layover and shadow are simulated [Meier et al., 1993]. From the sensor position, the DEM grid is sampled in range direction. Layover and shadow regions are detected analysing the distance and the viewing angle. By intersection of these results with the map data, the affected areas of buildings and roads are identified.

In order to find the best SAR parameters the simulations were systematically repeated with varying aspect angles α and viewing angles θ (Fig. 4). About 650 simulations have been carried out for the entire test site [Soergel et al, 2003b].

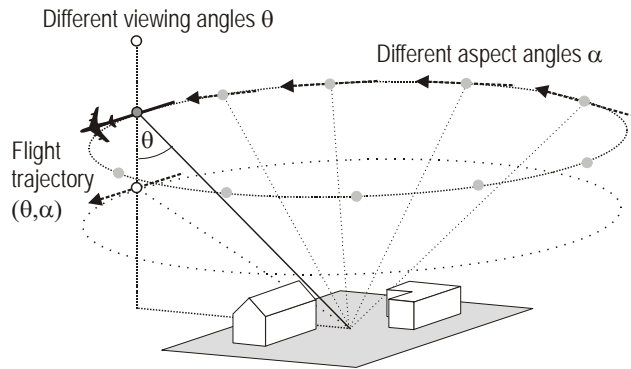


Fig. 4: Simulation of SAR phenomena layover and shadow

With the given sensor parameters, only 43% of the building roof area and about 20% of the road area can be sensed without distortions by layover and shadow. These numbers increase to 86% for roofs and 62% for roads in case of a combination of four chosen SAR acquisitions (Tab. 1).

| SAR measurements | 1 | 2 | 3 | 4 |
|-----------------------|------|------|------|------|
| Undistorted roof area | 51.6 | 72.8 | 81.5 | 86.5 |
| Undistorted road area | 39 | 47 | 55.6 | 62 |

Table 1. Portion of roof and road areas visible without distortions for several SAR acquisitions in per cent.

Two simulation results for the same area as shown in Fig. 3b are depicted in Fig. 5a,b. The first simulation was carried out with the parameters of the acquired InSAR data and the other one for an aspect angle from the right with same carrier altitude and viewing angle. The dependence of SAR data acquisition from the aspect angle can clearly be observed comparing e.g. the shadow and layover areas caused by the buildings *D* and *E*.

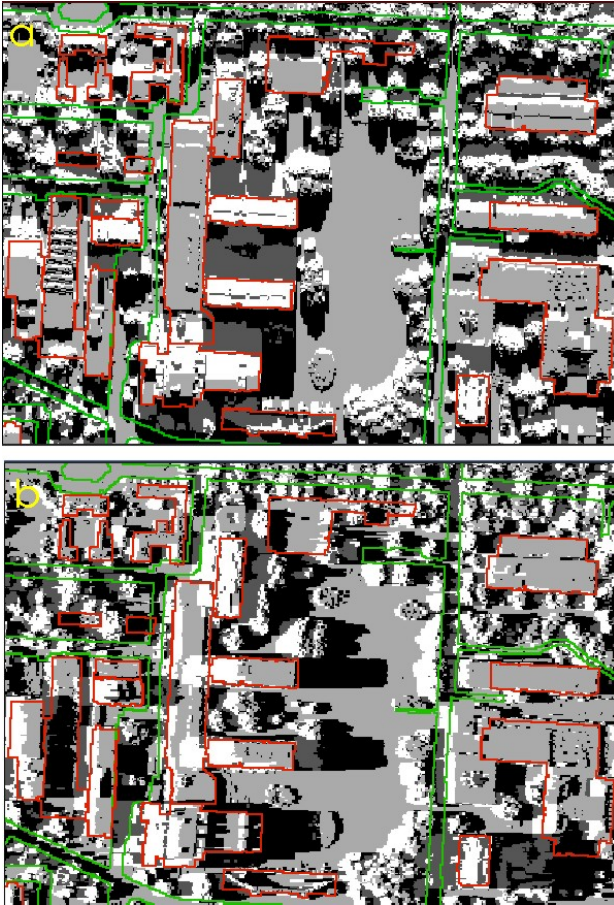


Fig. 5: a) simulation result for given SAR parameters (illumination from top): layover (white), shadow (black) layover and shadow (dark gray), and reliable data (bright gray) b) simulation for illumination from left.

5. ANALYSIS OF SAR DATA OF DENSE URBAN SCENES

The interpretation of SAR imagery in dense urban scenes without context information is often difficult even for experts. An important task in case of disaster monitoring is the detection of changes, e.g. damaged buildings and infrastructure. However, context information is usually not available for all areas at the same level. The benefit from integrating GIS data in the analysis will be discussed for different levels of available data in the GIS:

5.1 2D map data

In the simplest case the availability of a vector map containing a layer with building footprints is assumed. According to the sensor parameters, the building footprints can be transformed into the SAR images. The lack of height information leads to a shift of the transformed footprints similar to Fig. 3a. However, due to this shift the layover regions at the buildings are clearly visible. These areas could be e.g. excluded from the calculation of the building height from the InSAR DEM (Fig. 6b). The road layer of a vector map is useful for the discrimination of roads from cast shadow of buildings.

5.2 2D map data and mean building height

Using height information, the accuracy of the projected footprint positions is enhanced. Here, the mean height was determined by averaging the LIDAR data inside the building footprints. Fig. 6a shows the transformed footprints superimposed on the slant range magnitude image. The footprints of buildings, e.g. building D and E, are now correct. Due to the height difference, the two parts of building I appear at the same location in the SAR image.

The change detection capabilities for urban structures from SAR images can be demonstrated e.g. with buildings B and C. Some parts of these buildings are missing in the map (Fig. 3b), because they have been built after the map production. At the related SAR image positions, some building structures can be identified.

With the method described in section 4, layover and shadow areas can be predicted for the slant range geometry as well. The predicted shadow is useful for the discrimination between the cast shadow from buildings and other low backscatter areas like roads. By intersecting the road layer and the predicted layover areas, those bright objects on the road not coinciding with layover are hints to vehicles.

A further step is a simulation of SAR data. Because SAR images depend on the scene geometry and material properties, a complete simulation should address these features [Franceschetti et al., 1992]. But, usually detailed information about the materials e.g. of building roofs is not available. However, the image interpretation can benefit from simulations based on geometric properties alone. Fig. 6c shows the simulation result for the magnitude image. The appearance of the simulated and the acquired images differ noticeable, because besides the material properties the roof structures and the vegetation are not considered. Nevertheless, layover and occlusion areas are clearly visible.

5.3 LIDAR DEM

In order to reduce the deviations between the simulated and the acquired data, additional context knowledge is required. A high resolution LIDAR DEM provides information about the roof structure of the buildings. Furthermore, the vegetation impact of the object visibility in SAR data can be considered [Soergel, 2003a]. The wavelength dependency of the volume scattering inside tree or bush foliage can be taken into account by the choice of the suitable LIDAR data mode. For radar signals with short wavelength, first-pulse data is appropriate, while last-pulse data is advantageous in case of a larger radar wavelength. The simulation result depicted in Fig. 6d was based on the first-pulse DEM shown in Fig. 3b.

Comparing Fig. 6c and 6d, the influence of vegetation on the SAR mapping seems to be large even in urban areas. The signal contribution caused by the geometry of roof structures is now considered. The impact of material properties on the backscatter cannot be taken into account. Therefore, some buildings and the place in the middle appear darker in the acquired data. For example, a flat roof made of concrete shows up black in the magnitude image, because the signal is reflected away from the sensor at the smooth surface. Furthermore, the influence of dominant scattering is not covered with this kind of simulation. However, an image interpreter may benefit from such a visualization, e.g. for spotting damaged buildings.

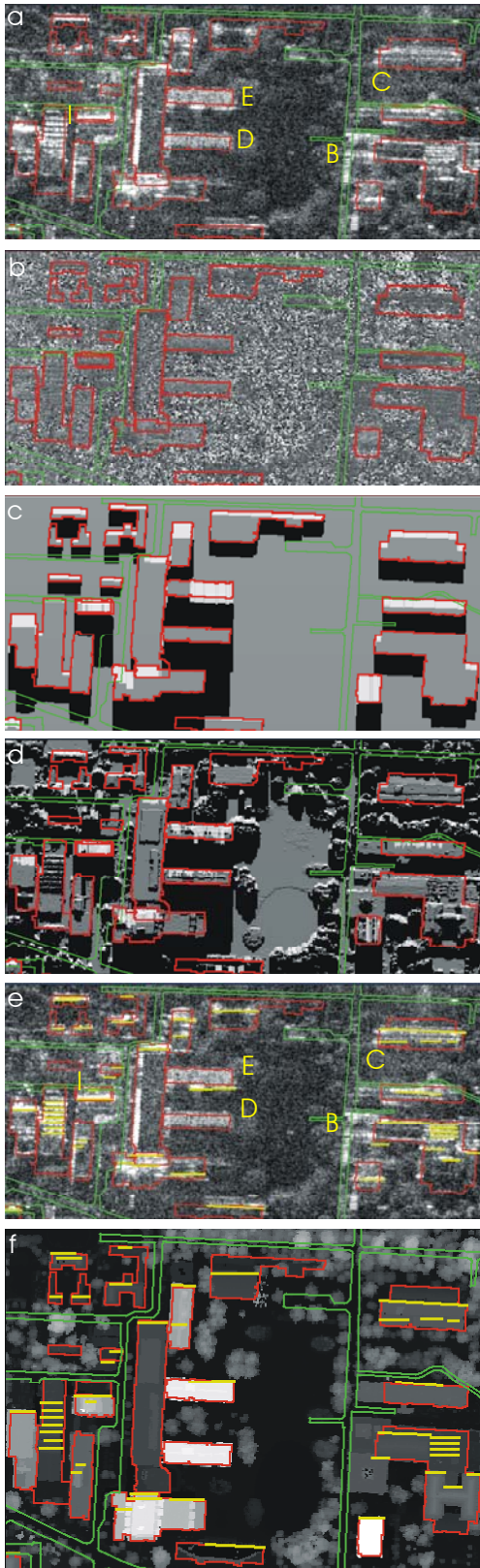


Fig. 6: a, b) slant range magnitude (a) and phase (b) image overlaid with footprints transformed using mean building height; b) simulation result based on building footprints and mean height; c) simulation result based on LIDAR DEM; d) image a) together with detected line scatterers (yellow); e) LIDAR DEM, map and line scatterers (yellow).

5.4 3D city model

In order to address salient line scatterers a vector representation of the object planes is required. Three dimensional city models provide such information. Here, the buildings were reconstructed using the LIDAR DEM and the building footprints [Stilla and Jurkiewicz, 1999].

From this vector data, possible locations of double-bounce effects and specular reflection are identified. In the first case, vertical building planes oriented towards the sensor are segmented. Building planes with a normal pointing to the sensor cause specular reflection. In both cases, occlusion from other objects in front is considered. The detected structures at building walls and roofs, e.g. the salient superstructures on buildings *B* and *J*, are shown in Fig. 6f. They match well with bright lines in the acquired data (Fig. 6e). The image interpreter may benefit in many ways from this kind of information. For example, the bright line below building *E* is actually caused by a double-bounce event and therefore located at the true position of the building footprint. The absence of predicted line scatterers or the appearances of additional ones are hints to changes in the scene. Furthermore, the polarimetric behaviour of the mapped objects can be predicted from the plane orientations e.g. of the building structures.

5.5 Fusion of multi-aspect SAR data

By a fusion of multi-aspect SAR data e.g. occlusion (shadow) areas can be filled and layover effects can be compensated. In general, the data fusion might be carried out at the iconic or the symbolic level. In the iconic case, often the orthorectified SAR imagery are fused, e.g. by choosing the brightest amplitude pixel or the DEM value with best coherence.

This method has some drawbacks. Firstly, if an InSAR DEM is used for orthorectification, straight object contours might not be mapped to straight lines on the ground, because of noise present in the DEM. Additionally, very high georeferencing accuracy is a prerequisite for such pixel-based fusion. Therefore, we recommend to carry out first the object segmentation in the slant range data, use this result for smoothing the InSAR DEM and to transform the symbolic description together with the related iconic 'texture' [Soergel et al., 2003c]. In such a way the mapping accuracy can be increased, by smoothing the InSAR DEM. For example, the maximum likelihood height estimate of a flat roofed building is the average of the corresponding DEM values. Secondly, an iconic fusion alone can hamper image interpretation, because object features like cast shadow areas might disappear. Hence, an additional fusion at the symbolic level seems to be advantageous.

With respect to the fusion of context data like maps and aerial images with SAR imagery we prefer the transformation of the reference data into the different slant range geometries and to superimpose it on the SAR data as shown above. In such a way linear structures can be compared with their slant range counterparts independently in each image.

6. CONCLUSION

In case of bad weather conditions or smoke, which do not allow taking useful data by aerial images or LIDAR a mapping using SAR is still possible. The side-looking illumination by SAR causes inherent artefacts particularly in dense urban areas. Usually some parts of the urban scene remain invisible using a single SAR data set. An analysis of multi-aspect SAR data offers an improvement of the results. The SAR acquisition

directions can be locally optimised, based on DEM and maps from a GIS.

Especially in dense urban areas, context information provided by GIS should be integrated in the analysis of SAR data. Particularly, high resolution DEM are useful for the mapping of the map data to the correct location in the data. The influence of the vegetation should not be neglected even in a dense urban environment. With a 3D vector representation of man-made objects, possible locations of strong scattering can be detected. Detailed information concerning the surface material of objects is usually not available. We recommend exploiting vector data of a 3D city model together with 3D raster data of the vegetation for the event-driven acquisition and analysis of SAR images.

ACKNOWLEDGMENT

We want to thank Prof. Dr. Ender and Dr. Brenner (FGAN-FHR Research Institute for High Frequency Physics and Radar Techniques) for providing the InSAR data acquired with the AER-II sensor (Ender, 1998).

REFERENCES

- Bamler, R., Schaettler, B., 1993. SAR Data Acquisition and Image Formation, in: G. Schreier (Ed.), SAR geocoding: data and systems, Wichmann Verlag, Karlsruhe, pp. 53-102.
- Dong, Y., Forster, B., Ticehurst, C., 1997. Radar Backscatter Analysis for Urban Environments, *Int. Journal of Remote Sensing*, Vol. 18, No. 6, pp. 1351-1364.
- Ender J.H.G., 1998. Experimental results achieved with the airborne multi-channel SAR system AER-II. *Proc. EUSAR'98*, pp. 315-318.
- Franceschetti, G., Migliaccio, M., Ricco, D., and Schrinzi, G., 1992. SARAS: A Synthetic Aperture Radar (SAR) Raw Signal Simulator, *IEEE Trans. Geosc. Remote Sensing*, Vol 30, 1, pp. 110-123.
- Gamba, P., Houshmand, B., Saccani, M., 2000. Detection and extraction of buildings from interferometric SAR data, *IEEE Transactions on Geoscience and Remote Sensing*, Vol. 38, No. 1, Part 2, pp. 611 –617.
- Guillaso, S., Ferro-Famil, L., Reigber, A., Pottier, E., 2003. Urban Area Analysis Based on ES-PRIT/MUSIC Methods using Polarimetric Interferometric SAR, *Proc. Urban, Berlin*, pp. 77-81.
- Kakumoto, S., Hatayama, M., Kameda, H., Taniguchi, T., 1997. Development of disaster management spatial information system. *Proc. GIS'97 Conf.*, pp. 595-598.
- Meier, E., Frei, U., Nuesch, D., 1993. Precise terrain corrected geocoded images. In G. Schreier (ed.), *SAR Geocoding: Data and Systems*: 173-185. Karlsruhe: Wichmann.
- Rosen, P. A., Hensley, S., Joughin, I. R., Li, F.K., Madsen, S. N., Rodriguez, E., Goldstein, R. M., 2000. Synthetic Aperture Radar Interferometry, *Proceed. of the IEEE*, 88, No. 3, pp. 333-382.
- Schreier, G., 1993. Geometrical properties of SAR images. In G. Schreier (ed.), *SAR geocoding: Data and Systems*: pp. 103-134. Karlsruhe: Wichmann.
- Shinozuka, M., Ghanem, R., Houshmand, B., Mansuri, B., 2000. Damage Detection in Urban Areas by SAR Imagery, *Journal of Engineering Mechanics*, Vol. 126, No. 7, pp. 769-777.
- Soergel, U., Schulz, K., Thoennessen, U., Stilla, U., 2003a. Event-driven SAR Data Acquisition in Urban Areas Using GIS, *GeoBIT/GIS Journal for Spatial Information and Decision Making*, Huethig Verlag, Heidelberg, Vol. 12, 2003, pp. 32-37.
- Soergel, U., Thoennessen, U., Stilla, U., 2003b. Visibility analysis of man-made objects in SAR images. 2nd GRSS/ISPRS Joint Workshop on Remote Sensing and data fusion on urban areas, URBAN 2003. *IEEE*, pp. 120-124.
- Soergel, U., Thoennessen, U., Stilla, U., 2003c. Reconstruction of Buildings from Interferometric SAR Data of built-up Areas, in: Ebner H, Heipke C, Mayer H, Pakzad K (eds) *Photogrammetric Image Analysis PIA. International Archives of Photogrammetry and Remote Sensing*. Vol. 34, Part 3/W8, pp. 59-64.
- Stilla, U., Jurkiewicz, K., 1999. Reconstruction of building models from maps and laser altimeter data. In: Agouris, P., Stefanidis, A. (eds.), *Integrated spatial databases: Digital images and GIS*: 34-46. Berlin: Springer.
- Stilla, U., Michaelsen, E., Soergel, U., Hinz, S., 2004. Airborne Monitoring of Vehicle Activity in Urban Areas. *International Archives of Photogrammetry and Remote Sensing*. Vol. 35, in press.
- Takeuchi, S., Suga, Y., Yonezawa, C., Chen, CH., 2000. Detection of urban disaster using InSAR - a case study for the 1999 great Taiwan earthquake. *Proc. IGARSS, CD ROM*.